Cell Labeling

International Edition: DOI: 10.1002/anie.201509601
German Edition: DOI: 10.1002/ange.201509601

Targeted Ultrasound-Assisted Cancer-Selective Chemical Labeling and Subsequent Cancer Imaging using Click Chemistry

Hua Wang, Marianne Gauthier, Jamie R. Kelly, Rita J. Miller, Ming Xu, William D. O'Brien, Jr., and Jianjun Cheng**

Abstract: *Metabolic sugar labeling followed by the use of reagent-free click chemistry is an established technique for in vitro cell targeting. However, selective metabolic labeling of the target tissues in vivo remains a challenge to overcome, which has prohibited the use of this technique for targeted in vivo applications. Herein, we report the use of targeted ultrasound pulses to induce the release of tetraacetyl N-azidoacetylmannosamine (Ac_4ManAz) from microbubbles (MBs) and its metabolic expression in the cancer area. Ac_4ManAz-loaded MBs showed great stability under physiological conditions, but rapidly collapsed in the presence of tumor-localized ultrasound pulses. The released Ac_4ManAz from MBs was able to label 4T1 tumor cells with azido groups and significantly improved the tumor accumulation of dibenzocyclooctyne (DBCO)-Cy5 by subsequent click chemistry. We demonstrated for the first time that Ac_4ManAz-loaded MBs coupled with the use of targeted ultrasound could be a simple but powerful tool for in vivo cancer-selective labeling and targeted cancer therapies.*

As an efficient method of incorporating chemical groups into cell-surface glycoproteins, metabolic labeling of unnatural sugars has been widely used for glycan visualization, glycoproteomics, and cell labeling.[1–3] Recently, researchers have shown increasing interest in applying it to cancer targeting by coupling with bioorthogonal chemistries.[4–6] In the first step, unnatural sugars with reactive chemical groups (such as azides) are delivered and metabolized in the cancerous tissues, followed by the targeted delivery of dibenzocyclooctyne (DBCO)-bearing therapeutics by the click chemistry in the second step. Despite being a two-step process, this strategy has several advantages in cancer targeting: 1) excellent targeting can be achieved by taking advantage of the rapid, highly efficient click chemistry; 2) receptor saturation and immunogenicity problems in conventional protein-based targeting strategies can be avoided by using manually installed chemical receptors;[7–9] and 3) small-molecule DBCO as targeting ligands can be easily incorporated into therapeutic agents or nanomedicines with tunable density. One key challenge in using this two-step strategy for in vivo cancer targeting is to specifically deliver the azido sugars to the cancerous tissues. Kim et al.[6] used chitosan nanoparticles to deliver azido sugars to cancers by taking advantage of the enhanced permeability and retention (EPR) effect of nanoparticles, but the targeting efficiency was very low with limited selectivity.

Ultrasound (US) imaging is widely used and recognized as a safe medical tool for disease diagnosis and treatment.[10–13] Microbubbles (MBs) that entrap gas in a biocompatible material to form micron-sized particles have achieved great success as US contrast agents (UCAs) owing to their high US reflectivity and great stability.[14] It is well established that high-amplitude US pressures cause expansion and contraction of MBs, resulting in their disruption.[15–17] A secondary effect of MB destruction is the temporary increase of capillary permeability and production of transient poration in cell membranes.[18–21] Researchers have reported the use of US pulses to burst MB–liposome conjugates and release the encapsulated drugs or genes specifically in the target tissues.[22–25] We envision that cancer-localized US pulses with accurate tissue targeting capability can potentially be used to induce the release of azido sugars from MBs specifically in the cancerous tissues.[26–28] Herein, we report the design of tetraacetyl *N*-azidoacetylmannosamine (Ac_4ManAz)-loaded MBs (Ac_4-MBs) for effective in vivo cancer-selective labeling (Scheme 1). In the presence of high-amplitude US pressures localized in the cancerous tissues, the MBs collapsed and released azido-sugar-loaded liposomes, and the temporarily increased capillary and cellular permeability facilitated the tumor penetration and cellular uptake of the released liposomes.[29–31] The released Ac_4ManAz then metabolically labeled the tumor cells with azido groups, which mediated targeted retention of DBCO-cargo for cancer imaging and potential cancer treatment.

Ac_4ManAz-loaded liposomes (Ac_4-lipo) functionalized with activated carboxylates were prepared by extrusion of the lipid mixture of hydrogenated L-α-phosphatidylcholine (HSPC), cholesterol, and 1,2-distearoyl-sn-glycero-3-phosphoethanolamine-*N*-[succinimidyl (polyethylene glycol)-2000] (DSPE-PEG_{2k}-NHS). The prepared Ac_4-lipo had a mean diameter of 180 nm and a sugar loading of 5.3% (w/w) (Figure 1a; Supporting Information, Figure S1). Ac_4-lipo showed excellent stability and minimal premature sugar release under physiological conditions (Figure S2). Amine-functionalized, perfluorobutane-gas-filled MBs with a mean diameter of 870 nm were prepared using the one-step

[*] H. Wang, M. Xu, Prof. Dr. J. Cheng
Department of Materials Science and Engineering
University of Illinois at Urbana-Champaign (USA)
M. Gauthier, J. R. Kelly, R. J. Miller, Prof. Dr. W. D. O'Brien, Jr.
Department of Electrical and Computer Engineering
University of Illinois at Urbana-Champaign
Urbana, IL 61801 (USA)
E-mail: wdo@uiuc.edu
jianjunc@illinois.edu

Supporting information for this article can be found under: http://dx.doi.org/10.1002/anie.201509601.

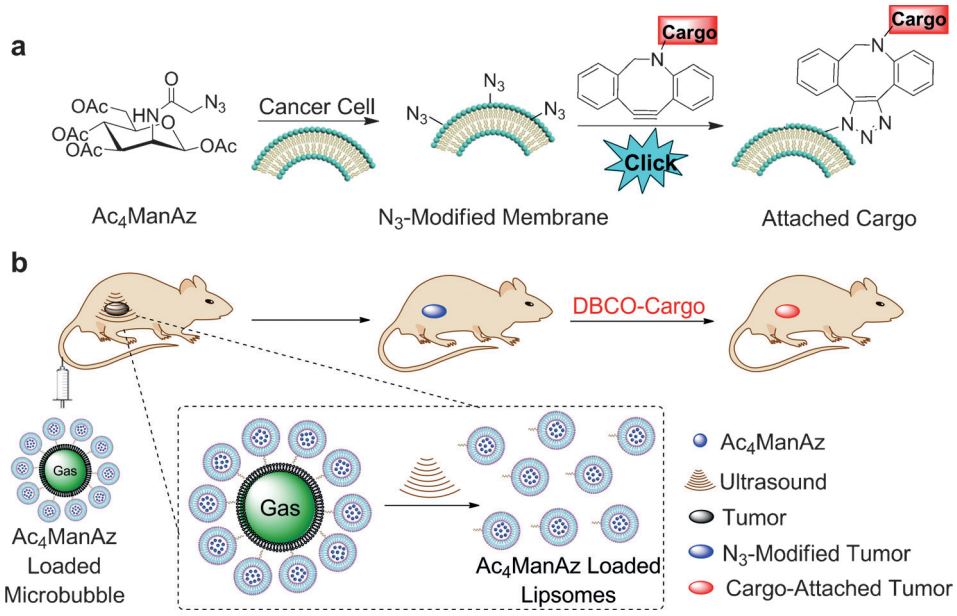

Scheme 1. a) Metabolic labeling of Ac_4ManAz and subsequent targeting of DBCO-cargo using copper-free click chemistry. b) Ultrasound-assisted accumulation and metabolic expression of Ac_4ManAz in the tumor area and subsequent tumor-targeted delivery of DBCO-cargo using click chemistry.

sonication method (Figure S2). Ac_4ManAz-loaded liposomes were then conjugated to MBs by the coupling reaction between activated carboxylates and amine groups. The resulting Ac_4-MB had a mean diameter of 1.03 μm and a narrow polydispersity index (PDI) of 0.22 (Figure 1b). Blank MB without Ac_4ManAz was prepared similarly (Figure S2). Ac_4-MB showed excellent stability under physiological conditions, as evidenced by the negligible change in diameter and number density over 6 days (Figure 1c). However, in the presence of high-amplitude US pressures, the MBs collapsed. The US pressures applied to collapse 5% and 50% of the Ac_4-MB population were 2.50 and 4.58 MPa, respectively (Figure 1d).

We next studied whether Ac_4-MB was able to metabolically label 4T1 breast cancer cells with azido groups when exposed to an US pressure field. 4T1 cells in Ac_4-MB containing medium were treated with US for 1 min, further incubated for 3 days, and then treated with DBCO-Cy5 for 1 h to detect the expression of azido groups. The cells without US treatment were used as a control. As shown in Figure 1e, minimal Cy5 fluorescence intensity (FI) was observed on the surface of 4T1 cells in the absence of US treatment, indicating the great stability and minimal premature sugar release of MBs during incubation. Because of its relatively large size, Ac_4-MB was unable to enter the 4T1 cells, and thus failed to release Ac_4ManAz in cells for metabolic labeling. In comparison, 4T1 cells exposed to high-amplitude US pressures showed strong Cy5 FI on the cell surface, suggesting that Ac_4-lipo were successfully released from the MBs, entered 4T1 cells through endocytosis, and released Ac_4ManAz for subsequent metabolic labeling of cells. Presumably, liposomes released the encapsulated azido sugars through fusion with cellular or intracellular membranes or by lytic degradation in the lysosomes.[32–35] We also tested the in vitro labeling kinetics of Ac_4-lipo by incubating it with 4T1 cells for different times, and subsequently detecting the cell-surface azido groups using DBCO-Cy5. As a result, Ac_4-lipo-mediated labeling of 4T1 cells was time-dependent, with the cell-surface azido density approaching a plateau value after 72–96 h (Figure S5).

After demonstrating in vitro that Ac_4-MB was able to metabolically label 4T1 breast cancer cells with azido groups only in the presence of US, we then went on to study whether targeted US pulses in the tumor area could be used to induce selective sugar labeling of tumor cells. As a proof-of-concept study, we first investigated whether targeted US in the tumor area could break intratumorally injected Ac_4-MB and induce metabolic labeling of tumor cells. Ac_4-MB was injected directly into the subcutaneous 4T1 tumors on the flanks of BALB/c mice with simultaneous treatment of targeted US. The right tumors were treated with high-amplitude US pressure pulses (the US system output was set to the 100% to collapse the MBs), while the left tumors were treated with low-amplitude US pressure pulses (the US system output was 4%, so that the MBs would not collapse and yet still provide US imaging capability; Figure S7a, S7b). Ac_4-MB injected into the right tumors collapsed and rapidly diffused away during injection in the presence of 100% US (upper panel, Figure 2). In comparison, most of Ac_4-MB injected into the left tumors with 4% US treatment remained intact and deposited near the injection site (lower panel, Figure 2). Western blot analyses of tumor tissues at 72 h post injection (p.i.) of Ac_4-MB showed the existence of more azido-modified protein bands in the right tumors treated with 100% US than in the left tumors treated with 4% US (Figure S7c), suggesting the enhanced metabolic labeling of tumor cells in the presence of high-amplitude US pressure.

To understand how the enhanced azido expression in the right tumors would improve the tumor accumulation of DBCO-cargo through the click reaction, in a separate study, DBCO-Cy5 was intravenously (i.v.) injected via the tail vein, and its biodistribution was monitored by in vivo fluorescence imaging. At 24 or 48 h p.i. of DBCO-Cy5, a distinct difference in Cy5 FI between the right tumors treated with 100% US and left tumors treated with 4% US was observed (Figures 3a and S7d), while mice injected with blank MB showed negligible difference in Cy5 FI between the right and left tumors (Figures 3a and S7d). Ex vivo fluorescence imaging showed a 1.35-fold Cy5 FI in the right tumor compared to the left tumor in Ac_4-MB group (Figure 3b). In comparison,

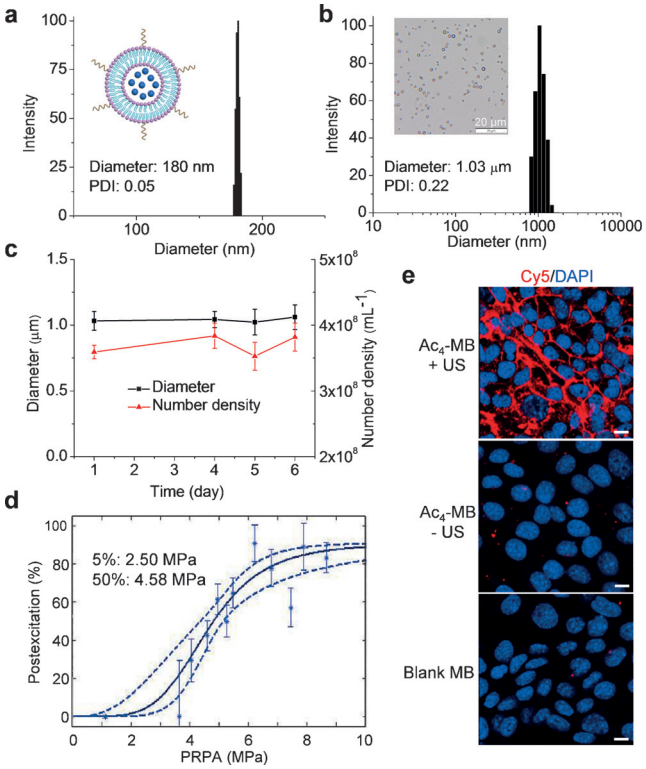

Figure 1. a) Diameter and diameter distribution of Ac_4ManAz-loaded liposome. b) Diameter and diameter distribution of Ac_4-MB. Inset: microscopic image of Ac_4-MB. c) Change of diameter and number density of Ac_4-MB over time in 10% fetal bovine serum. d) Percentage post-excitation (collapse) curve for Ac_4-MB, plotted against peak rarefactional pressure amplitude (PRPA). e) CLSM images of 4T1 cells after treatment with Ac_4-MB, with or without one-minute US treatment for three days, followed by labeling with DBCO-Cy5 for 1 h. Cells treated with blank MB and labeled with DBCO-Cy5 were used as control. The cell nucleus was stained with DAPI (blue). Scale bar = 10 μm.

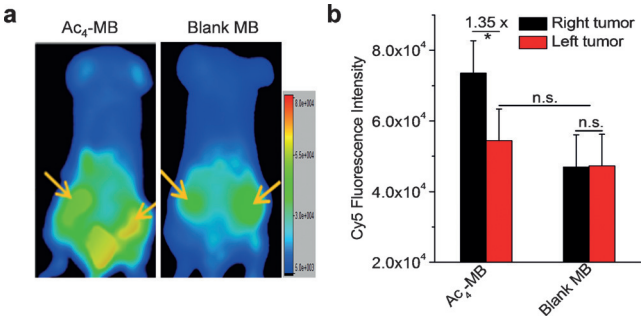

Figure 3. a) In vivo whole body fluorescence imaging of BALB/c mice pretreated with Ac_4-MB and blank MB, respectively, at 48 h p.i. of DBCO-Cy5. b) Ex vivo FI of tumors from BALB/c mice pretreated with Ac_4-MB and blank MB, respectively, at 48 h p.i. of DBCO-Cy5. Data are presented as mean ± SEM ($n = 3$) and analyzed by one-way ANOVA (Fisher; $0.01 < {*}P \le 0.05$; ${**}P \le 0.01$; ${***}P \le 0.001$).

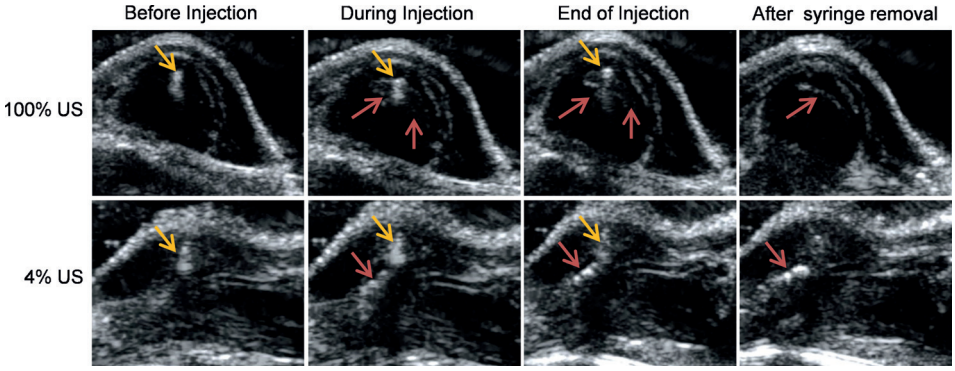

Figure 2. US imaging of the tumor area of BALB/c mice during the intratumoral injection of Ac_4-MB. 100% and 4% US was applied to the right and left tumors, respectively, upon MB injection (1 min), and continuously applied for another 1 min after MB injection. The yellow arrow indicates the syringe, and the red arrow indicates the MBs.

negligible difference in Cy5 FI between the right and left tumors was observed in the blank MB group (Figure 3b). It is noteworthy that the left tumors of Ac_4-MB group with 4% US treatment showed a statistically non-significant change of Cy5 FI compared to the tumors of the blank MB group (Figure 3b), suggesting the good stability of Ac_4-MB in the tumor environment. Confocal images of the right tumor sections also showed much stronger Cy5 FI than the left tumor sections in Ac_4-MB group (Figure S7h). These findings demonstrate that targeted US pressure in the tumor area collapsed the intratumorally injected Ac_4-MB and facilitated the release and metabolic expression of Ac_4ManAz. The expressed azido groups were able to significantly enhance the tumor accumulation of DBCO-Cy5 through the efficient click reaction.

After demonstrating that targeted US was able to collapse intratumorally injected Ac_4-MB, we next investigated whether targeted US in the tumor area could collapse Ac_4-MB that was injected systemically and subsequently induce the tumor accumulation and metabolic expression of Ac_4ManAz. BALB/c mice bearing subcutaneous 4T1 tumors were divided into four groups: Ac_4-MB with US treatment on the left tumors (Group 1); blank MB with US treatment on the left tumors (Group 2); Ac_4-MB without US treatment (Group 3); and PBS without US treatment (Group 4). MB injections and targeted US exposures were given once daily for three days (Days 1, 2, and 3). DBCO-Cy5 was i.v. injected on Day 4 and its biodistribution was monitored by in vivo fluorescence imaging (Figure 4a). As shown in Figure 4b, a clear Cy5 fluorescence contrast between the left tumors with US treatment and the right tumors without US treatment was observed in Group 1 mice at 24 and 48 h p.i. of DBCO-Cy5. In comparison, a negligible difference in the DBCO-Cy5 signal between the left and right tumors was observed in Group 2 mice without the sugar treatment, and in Group 3 mice

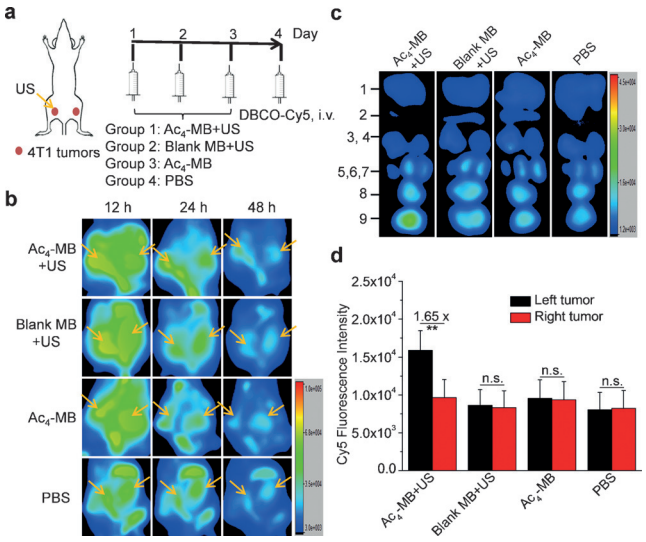

Figure 4. a) Time frame of in vivo imaging study. When 4T1 tumors in both flanks of BALB/c mice reached a diameter of approximately 5 mm, the hair over the tumor area was shaved and depilated, and Ac_4-MB (50 mg kg^{-1} in sugar equivalent) or blank MB (same amount of MB) was i.v. injected with simultaneous US exposures on the left tumors once daily for three days. On Day 4, DBCO-Cy5 (5 mg kg^{-1}) was i.v. injected. b) In vivo whole body fluorescence imaging of BALB/c mice at 12, 24, and 48 h p.i. of DBCO-Cy5, respectively. c) Ex vivo imaging of tumors and major organs at 48 h p.i. of DBCO-Cy5. 1-liver, 2-spleen, 3-lung, 4-brain, 5-heart, 6,7-kidneys, 8-right tumor, 9-left tumor. d) Quantification of Cy5 FI in tumors from (c). Data are presented as mean ± SEM ($n = 3$) and analyzed by one-way ANOVA (Fisher; $0.01 < *P \leq 0.05$; $**P \leq 0.01$; $***P \leq 0.001$).

without the US treatment. Ex vivo imaging showed a 1.65-fold Cy5 FI in the left tumors compared to the right tumors in Group 1 mice, with no significant difference in Cy5 FI between the left and right tumors observed in all other groups (Figure 4c,d). In comparison, healthy organs, including the liver, spleen, lung, brain, heart, and kidney, showed negligible differences for the amount of retained Cy5 among all groups (Figure S8b, S8c). These findings demonstrated that targeted US could improve the accumulation and expression of Ac_4ManAz specifically in the tumor area, presumably as a result of the easier tumor penetration of released Ac_4-lipo in the presence of the US exposure. In comparison with the three-injection regimen, mice administered with one i.v. injection of Ac_4-MB showed a 1.16-fold accumulation of DBCO-Cy5 in the left tumors with US treatment compared to the right tumors without US treatment (Figure S9), which suggested that azido labeling of tumors and subsequent tumor targeting of DBCO-cargo could be further improved by increasing the dose of Ac_4-MB.

To further understand the benefits of the two-step targeting strategy of Ac_4-MB and click chemistry, we evaluated the tumor targeting efficiency of Cy5-labeled MB (Cy5-MB) in the presence of tumor-targeted US. BALB/c mice bearing subcutaneous 4T1 tumors were i.v. injected with Cy5-MB, with simultaneous US treatment on the left tumors. The right tumors without US treatment were used as controls. At 48 h p.i. of Cy5-MB, ex vivo imaging of harvested tissues showed a statistically non-significant change of Cy5-MB accumulation between the left and right tumors (Figure S10), in sharp contrast to the 1.65-fold tumor targeting efficiency achieved by the combinational strategy of Ac_4-MB and DBCO-Cy5 (Figure 4d). In addition, the vast majority of Cy5-MB accumulated in liver and lung, showing an extremely low tumor-to-organ accumulation ratio (Figure S10). These experiments validated that Ac_4-MB coupled with DBCO-cargo can not only mediate a much higher cancer-targeting efficiency than cargo-loaded MB, but also enables the choice of cargo-delivery systems with more favorable pharmacokinetics than MB. In another set of experiments, we i.v. injected Ac_4-MB into BALB/c mice once daily for three days with simultaneous US treatment on the right thigh muscles, and then i.v. injected DBCO-Cy5. At 48 h p.i. of DBCO-Cy5, the right thigh muscles with US treatment failed to show an increase of DBCO-Cy5 accumulation compared to the left thigh muscles without US treatment (Figure S11), which together with the achieved 1.65-fold tumor-targeting effect (Figure 4d), suggested that sugar expression in cancerous tissues was more favored than in normal tissues.

In summary, we developed Ac_4-MB for cancer-targeted labeling and imaging with the assistance of targeted US. Targeted US pulses could induce the collapse of Ac_4-MB (while being visualized under US imaging) and the release and metabolic expression of azido sugars within the tumor, which significantly increased the tumor accumulation of DBCO-Cy5 by 65% through the click reaction compared to the group without US treatment. More importantly, the accumulation of DBCO-Cy5 in healthy tissues showed negligible changes. In contrast to antibody–drug conjugate[36] and nanoparticle–ligand conjugate[37–40] targeting strategies, which improve the cellular uptake instead of the overall tumor–organ accumulation ratio of drugs or drug delivery systems, our strategy can intrinsically enhance the tumor–organ accumulation ratio of therapeutic agents. Ac_4-MB coupled with the use of targeted US could be a simple but powerful tool for in vivo cancer targeting and targeted cancer therapies.

Acknowledgements

This work was supported by NIH (Director's New Innovator Award 1DP2OD007246), NSF (DMR 1309525) and NIH (R37EB002641). H. Wang is funded by Howard Hughes Medical Institute International Student Research Fellowship.

Keywords: cell labeling · click chemistry · drug design · sugars · ultrasound

How to cite: *Angew. Chem. Int. Ed.* **2016**, *55*, 5452–5456
Angew. Chem. **2016**, *128*, 5542–5546

[1] S. T. Laughlin, N. J. Agard, J. M. Baskin, I. S. Carrico, P. V. Chang, A. S. Ganguli, M. J. Hangauer, A. Lo, J. A. Prescher, C. R. Bertozzi, *Methods in Enzymology, Vol. 415*, Academic Press, New York, **2006**, p. 230.
[2] J. A. Prescher, D. H. Dube, C. R. Bertozzi, *Nature* **2004**, *430*, 873.
[3] S. T. Laughlin, J. M. Baskin, S. L. Amacher, C. R. Bertozzi, *Science* **2008**, *320*, 664.

[4] H. Koo, S. Lee, J. H. Na, S. H. Kim, S. K. Hahn, K. Choi, I. C. Kwon, S. Y. Jeong, K. Kim, *Angew. Chem. Int. Ed.* **2012**, *51*, 11836; *Angew. Chem.* **2012**, *124*, 12006.
[5] K. Fukase, K. Tanaka, *Curr. Opin. Chem. Biol.* **2012**, *16*, 614.
[6] S. Lee, H. Koo, J. H. Na, S. J. Han, H. S. Min, S. J. Lee, S. H. Kim, S. H. Yun, S. Y. Jeong, I. C. Kwon, K. Choi, K. Kim, *ACS Nano* **2014**, *8*, 2048.
[7] M. Khazaeli, R. M. Conry, A. F. LoBuglio, *J. Immunol.* **1994**, *15*, 42.
[8] P. Chames, M. Van Regenmortel, E. Weiss, D. Baty, *Br. J. Pharmacol.* **2009**, *157*, 220.
[9] F. J. Esteva, *Oncologist* **2004**, *9*, 4.
[10] F. H. Rose, C. D. McGregor, P. Mathur, US Patent 4, 896, 673, **1990**.
[11] C. M. Rumack, S. R. Wilson, J. W. Charboneau, *Diagnostic ultrasound*, *Vol. 2*, Mosby, **1998**.
[12] A. Heimdal, A. Støylen, H. Torp, T. Skjærpe, *J. Am. Soc. Echocardiogr.* **1998**, *11*, 1013.
[13] W. D. O'Brien, Jr., *Prog. Biophys. Mol. Biol.* **2007**, *93*, 212.
[14] J. R. Lindner, *Nat. Rev. Drug Discovery* **2004**, *3*, 527.
[15] J. P. Christiansen, B. A. French, A. L. Klibanov, S. Kaul, J. R. Lindner, *Ultrasound Med. Biol.* **2003**, *29*, 1759.
[16] R. Bekeredjian, S. Chen, P. A. Frenkel, P. A. Grayburn, R. V. Shohet, *Circulation* **2003**, *108*, 1022.
[17] Q. Lu, H. Liang, T. Partridge, M. Blomley, *Gene Ther.* **2003**, *10*, 396.
[18] P. Prentice, A. Cuschieri, K. Dholakia, M. Prausnitz, P. Campbell, *Nat. Phys.* **2005**, *1*, 107.
[19] M. Kinoshita, N. McDannold, F. A. Jolesz, K. Hynynen, *Proc. Natl. Acad. Sci. USA* **2006**, *103*, 11719.
[20] L. H. Treat, N. McDannold, N. Vykhodtseva, Y. Zhang, K. Tam, K. Hynynen, *Int. J. Cancer* **2007**, *121*, 901.
[21] M. M. Forbes, W. D. O'Brien, *J. Acoust. Soc. Am.* **2012**, *131*, 2723.
[22] S.-L. Huang, *Adv. Drug Delivery Rev.* **2008**, *60*, 1167.
[23] R. Suzuki, T. Takizawa, Y. Negishi, K. Hagisawa, K. Tanaka, K. Sawamura, N. Utoguchi, T. Nishioka, K. Maruyama, *J. Controlled Release* **2007**, *117*, 130.
[24] K. Ferrara, R. Pollard, M. Borden, *Annu. Rev. Biomed. Eng.* **2007**, *9*, 415.
[25] R. Suzuki, E. Namai, Y. Oda, N. Nishiie, S. Otake, R. Koshima, K. Hirata, Y. Taira, N. Utoguchi, Y. Negishi, *J. Controlled Release* **2010**, *142*, 245.
[26] C. J. Pavlin, K. Harasiewicz, M. D. Sherar, F. S. Foster, *Ophthalmology* **1991**, *98*, 287.
[27] G. S. Rozycki, M. G. Ochsner, J. H. Jaffin, H. R. Champion, *J. Trauma Acute Care Surg.* **1993**, *34*, 516.
[28] D. H. O'Leary, J. F. Polak, S. Wolfson, M. G. Bond, W. Bommer, S. Sheth, B. M. Psaty, A. R. Sharrett, T. A. Manolio, *Stroke* **1991**, *22*, 1155.
[29] K. E. Hitchcock, D. N. Caudell, J. T. Sutton, M. E. Klegerman, D. Vela, G. J. Pyne-Geithman, T. Abruzzo, P. E. Cyr, Y.-J. Geng, D. D. McPherson, *J. Controlled Release* **2010**, *144*, 288.
[30] A. Schroeder, J. Kost, Y. Barenholz, *Chem. Phys. Lipids* **2009**, *162*, 1.
[31] A. Schroeder, R. Honen, K. Turjeman, A. Gabizon, J. Kost, Y. Barenholz, *J. Controlled Release* **2009**, *137*, 63.
[32] R. Agarwal, I. Iezhitsa, P. Agarwal, N. A. Abdul Nasir, N. Razali, R. Alyautdin, N. M. Ismail, *Drug Delivery* **2014**, 1.
[33] R. Mo, T. Jiang, Z. Gu, *Angew. Chem. Int. Ed.* **2014**, *53*, 5815; *Angew. Chem.* **2014**, *126*, 5925.
[34] S. R. Paliwal, R. Paliwal, G. P. Agrawal, S. P. Vyas, *Nanomedicine* **2011**, *6*, 1085.
[35] H. Wang, T. Peters, A. Sindrilaru, K. Scharffetter-Kochanek, *J. Invest. Dermatol.* **2009**, *129*, 1100.
[36] D. B. Kirpotin, D. C. Drummond, Y. Shao, M. R. Shalaby, K. Hong, U. B. Nielsen, J. D. Marks, C. C. Benz, J. W. Park, *Cancer Res.* **2006**, *66*, 6732.
[37] O. C. Farokhzad, J. Cheng, B. A. Teply, I. Sherifi, S. Jon, P. W. Kantoff, J. P. Richie, R. Langer, *Proc. Natl. Acad. Sci. USA* **2006**, *103*, 6315.
[38] J. Cheng, B. A. Teply, I. Sherifi, J. Sung, G. Luther, F. X. Gu, E. Levy-Nissenbaum, A. F. Radovic-Moreno, R. Langer, O. C. Farokhzad, *Biomaterials* **2007**, *28*, 869.
[39] L. Tang, X. Yang, L. W. Dobrucki, I. Chaudhury, Q. Yin, C. Yao, S. Lezmi, W. G. Helferich, T. M. Fan, J. Cheng, *Angew. Chem. Int. Ed.* **2012**, *51*, 12721; *Angew. Chem.* **2012**, *124*, 12893.
[40] Z. Cao, R. Tong, A. Mishra, W. Xu, G. C. L. Wong, J. Cheng, Y. Lu, *Angew. Chem. Int. Ed.* **2009**, *48*, 6494; *Angew. Chem.* **2009**, *121*, 6616.

Received: October 13, 2015
Revised: January 29, 2016
Published online: March 24, 2016

